This is a repository copy of *Nanoparticles enabled pump-free direct absorption solar collectors*.

White Rose Research Online URL for this paper:
http://eprints.whiterose.ac.uk/155104/

Version: Accepted Version

Article:

Jin, H, Lin, G, Guo, Y et al. (2 more authors) (2020) Nanoparticles enabled pump-free direct absorption solar collectors. Renewable Energy, 145. pp. 2337-2344. ISSN 0960-1481

https://doi.org/10.1016/j.renene.2019.07.108

Nanoparticles enabled pump-free direct absorption solar collectors

Haichuan Jin[1], Guiping Lin[1], Yuandong Guo[1], Lizhan Bai[1], Dongsheng Wen[*,1,2]

[1]Laboratory of Fundamental Science on Ergonomics and Environmental Control, School of
Aeronautic Science and Engineering, Beihang University, Beijing 100191, PR China
[2]School of Chemical and Process Engineering, University of Leeds, Leeds, LS2 9JT, UK
Corresponding Author: Dongsheng Wen, Email: d.wen@buaa.edu.cn

Abstract: Developing renewable energy technologies, especially solar energy-based, is of great importance to secure our energy future. Current solar thermal systems, however, have relatively low utilization efficiencies, limited not only by their low solar energy capture efficiency but also the auxiliary pumping power to circulate the working fluid. Here an innovative nanoparticle enabled pump-free direct absorption solar collector concept is presented, which combines the advantages of volumetric solar harvesting and oscillating heat pipes. Two different flow modes have been observed when the concentration of nanofluid is different. There is an optimum filling ratio when the thermal resistance reaches the minimum. Validation experiments show that the proposed concept can efficiently harvest solar energy and spontaneously transfer the heat into targeted areas, providing a novel approach for efficient solar energy utilization.

Keywords: solar energy, nanoparticles, energy efficiency, volumetric solar harvesting, oscillating heat pipe

1. Introduction

Developing renewable and sustainable energy technologies, especially solar energy-based, is of great importance to secure our energy future [1]. Among different solar applications including photovoltaics and photocatalysis, solar thermal system (STS), i.e., direct conversion of solar energy to heat, still occupies the largest share [2]. Improving the system's energy utilization efficiency is crucial for its further large scale development [3]. In a typical STS, an engineered surface is utilized as the solar absorber where solar radiation is converted into heat, which is transferred to a working fluid flowing in the tubes embedded within or welded onto the surface. In such a system, the efficiency is limited by not only how efficiently the solar absorber captures the solar radiation, but also how effectively the heat is transferred to the working fluid [4]. It is a surface-controlled heat transfer process where the highest temperature is on the absorber surface and the lowest temperature is in the center of the fluid [5], resulting in high heat loss and large thermal resistance. In addition, large pumping power is required to drive the fluid circulation, which further increases the auxiliary work of the system.

One recent development to improve the performance of a STS is to use direct absorption nanofluids, i.e. to change the surface-based heat transfer mode to a volumetric one by seeding nanoparticles inside the heat transfer fluid [6–8]. As typical fluids such as water, solar oil or molten salts have low absorptive properties over the solar spectrum, seeding nanoparticles that can absorb solar energy directly within the fluid volume, the so-called direct absorption solar collector (DASC), becomes very attractive [9–11]. The solar energy conversion efficiency could be significantly improved by engineering solar absorption spectrum at the nanoscale [5,12–14], leading to much simplified and compact design. Many experimental studies have shown that by introducing certain nanoparticles (Ag, Au, Cu, carbon, etc.) into heat transfer fluids, the solar

collector efficiency can be improved significantly compared to the conventional ones [15]. Among the nanomaterials investigated, gold nanoparticle has attracted intensive interest due to its Surface Plasmon Resonance effects (SPR) [16,17]. Some pilot studies have shown that DASC could be a promising alternative to conventional solar collectors [18–21].

As a promising heat transfer concept first proposed in the 1990's [22], OHP has the advantage of simple structure, low cost, high flexibility and excellent heat transfer performance [23,24]. OHP is made of a long capillary tube bent into many turns, and fluid circulation is driven by bubble expansion at the evaporator section and contraction at the condenser section, without the requirement of additional pumping power. Currently in some OHP studies, capillary tubes are made of metals [25,26] and some are made of transparent materials [27] for 'flow visualization' purpose. Some researchers have tried to use OHP for transferring solar energy [28–30]. However, solar irradiation is not the direct heat source for almost all these studies, i.e., the surface of the plate solar collector absorbs the radiative energy, and the OHP transfers the harvested thermal energy from the collector to somewhere else. The whole efficiency of the system still surfers from the ill-suited heat transfer process, where the heat generation is separated form the fluid to be heated. The new concept that combines the advantage of DASC (which efficiently absorbs solar energy) and OHP (which efficiently transfers thermal energy) has not been proposed.
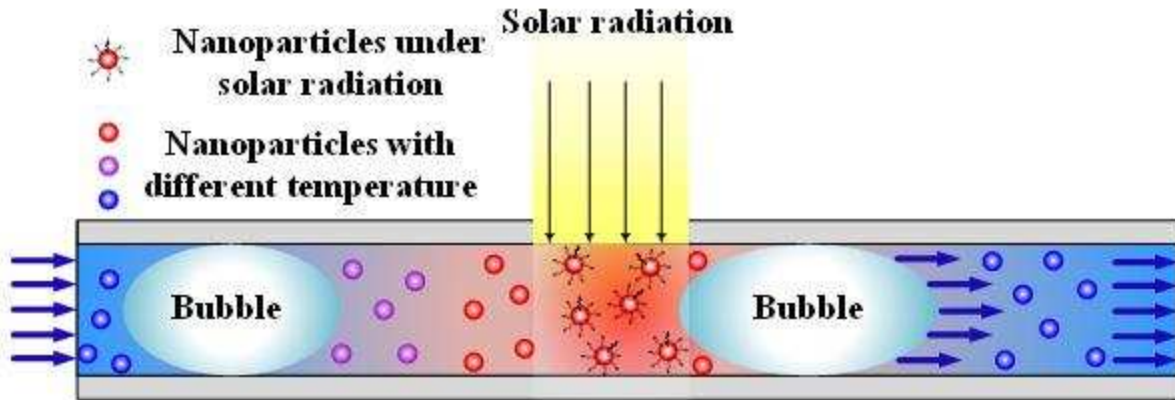
Fig. 1 Conceptive view of pump-less direct absorption solar collector

This work proposes an innovative pump-free DASC concept by using oscillating bubbles (OB), as shown in **Fig. 1**. Different to other capillary or gravity-driven solar collectors [31,32], fluids circulation and heat transport between the hot and cold sinks are driven by oscillating bubbles, i.e., a concept used in oscillating heat pipes (OHP) that have shown some promise in improving the performance of conventional solar collectors [30,33]. In the innovative concept, direct-absorption nanoparticles are dispersed into a base liquid enclosed by transparent capillary tubes. The particles absorb solar energy directly within the fluid (i.e. evaporator) under solar radiation and generate confined bubbles, which push the liquid to a condenser where heat is released. Such a concept has many distinctive features such as volumetric absorption, no need of pump, and light/compact design, which could lead to next generation of high efficiency solar collectors.

2. Experimental setup
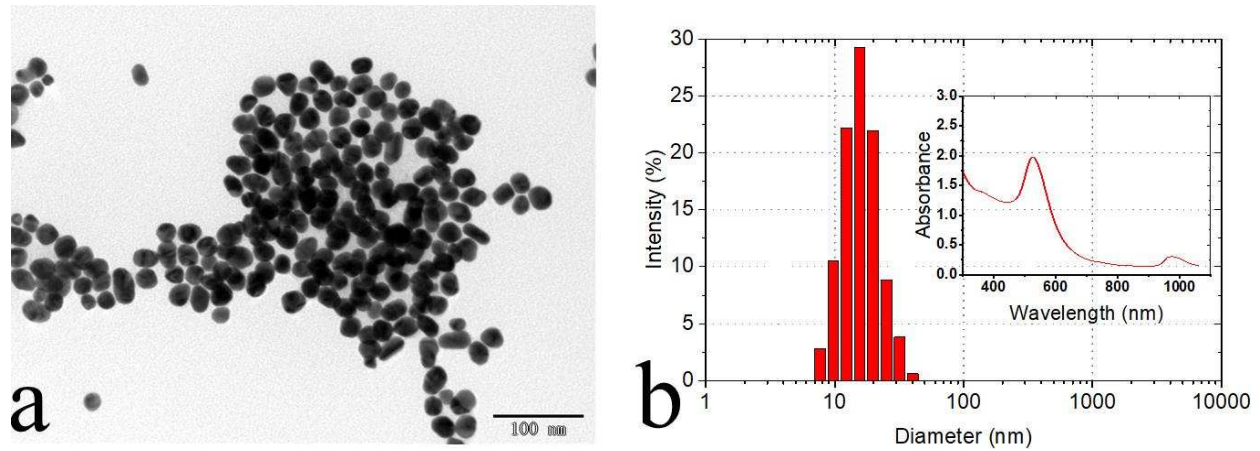
Fig. 2 (**a**) TEM image for AuNPs. (**b**) Particle size distribution and UV-Vis result (inset) of gold nanofluid with a concentration of 5 ppm

Au nanoparticles (AuNPs) have been reported to have strong solar absorption, and they were selected for the preparation of different nanofluids as the working fluids of the OHP. The one-step method [34] was employed to produce stable AuNPs nanofluids. Briefly 5×10^{-6} mol HAuCl$_4$ was first dispersed into 190 ml DI water in a three-necked flask. A magnetic blender with a heating source was used to stir the liquid until boiling. Boiling was continued for 10 mins and 10 ml of 0.5% sodium citrate was subsequently added. The solution turned dark blue within 30 s and the final color became wine red after being heated for an additional 20 mins. The dispersions maintained good stability for over two months and were used for the experiments without further purification and separation. Particles' size and shape were characterized (**Fig. 2a**) by a Transmission Electron Microscopy (TEM) (Tecnai G2 F20 S-TWIN). The optical property of gold nanofluids was characterized by a UV-spectrophotometer (Shimadzu UV-1800). A dynamic light scattering (DLS) device (Malvern nanosizer) was employed to identify the particle size distribution, which can be seen from **Fig. 2b**.
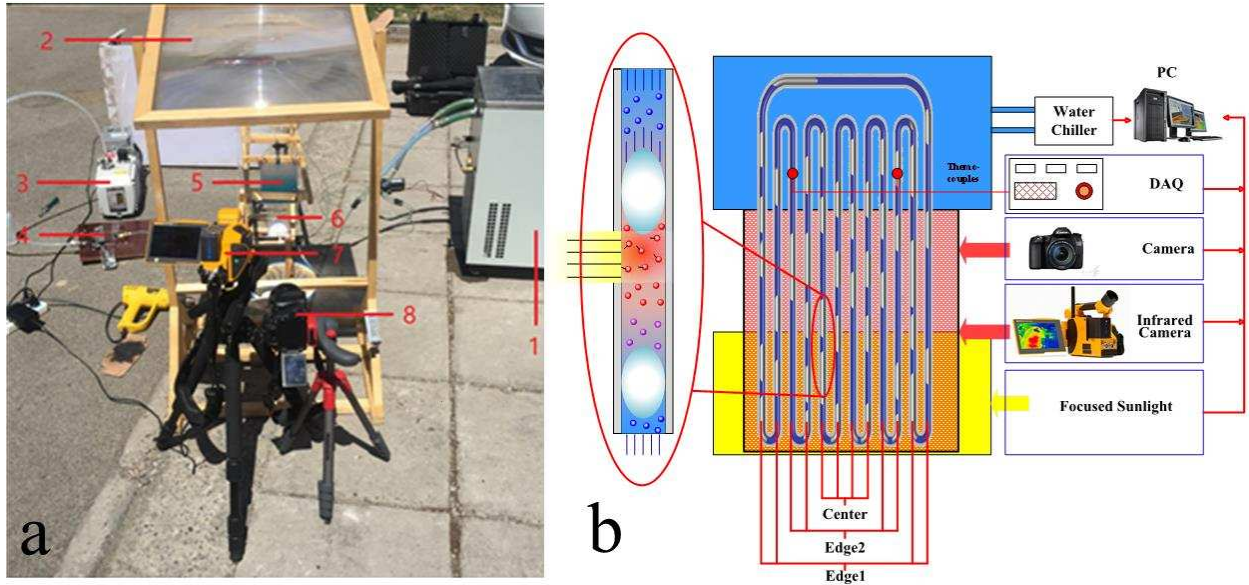
Fig. 3 (**a**) Experimental setup for investigating the performance of solar absorber with constant temperature of condenser: 1.Water chiller producing circulation cooling water with a constant temperature of 15 ℃; 2. Fresnel lens with dimension of 0.5 m × 0.5 m; 3. Vacuum pump; 4. Charging pipeline for OHPs; 5. Cooling water container maintaining constant temperature of the condenser of solar absorber; 6. OHP; 7. Infrared camera; and 8. High-speed camera. (**b**) Schematic of the experimental system, where the number for each pipe is named 1 to 12 from left to right

A feasibility study is conducted in this work to validate the concept. In the experiment, water is used as the base fluid, and gold nanoparticles are used as the direct absorption agencies. A 12-turn transparent oscillating heat pipe is designed and the new concept is examined under a solar concentration of 500 times, as shown in **Fig. 3**. OHPs were made from high temperature resistant quartz glass with pipe diameter of 2 mm with gap between two adjacent pipes, where the number for each pipe is named 1 to 12 from left to right, as shown in **Fig. 3b**. The average temperature of evaporation section of pipe number 1, 2, 11, 12 is named as **Edge1**. The average temperature of pipe number 3, 4, 9, 10 is named as **Edge 2**. The average temperature of pipe number 5~8 is named

as **Center**, as shown in **Fig. 3b**. The inner diameter (Di) was determined from Liu and Zhao etc. [35]. A typical inner diameter of 2 mm with the length of pipes of 200 mm was chosen in the experiment. The condensation section of OHP was cooled by circulating water with a constant temperature of 15 ℃ produced by a water chiller (SKD Refrigeration). As shown in **Fig. 3a**, Fresnel lens (Shenzhen MEIYING Technology CO., LTD.) with 100 cm focal distance was used to focus the sunlight to 500 times. A high precision infrared camera (Fluke Tix 640 with 30 mm lens) was used to capture the temperature distribution of DAS-OHPs. In order to record the bubble generation and acceleration process, a high-performance camera (Cannon 70D with 18-135 mm lens) was used. The schematic of the experimental system can be seen in **Fig. 3b**.

Three type K thermocouples with precision of ± 0.1℃ (Omega 5TC-TT-K-30-36) were connected to a data acquisition system (National Instruments PIXe-1073). Two of the thermocouples were used to measure the temperature change of water with thermal insulation for cooling the condenser of the OHP (**Fig. 3**). One thermocouple was used to measure the ambient temperature change during the experiment. A solar radiation intensity sensor with a measurement uncertainty of 2.0% was employed to measure the solar intensity.

All the experiments were conducted on 30th April 2017 (Beihang University, Beijing, China, location: 39° 59' 5.49" North, 116° 21' 18.70" East) from 10.00 am to 15.00 pm. As shown in **Fig. 4a**, the solar intensity varied from 870~1000 W/m^2, the ambient temperature varied from 33~38 ℃ during the experiment, which was relatively stable for the current experimental setting. The position of OHPs were precisely controlled so that the solar intensity distribution of each experiments was approximately the same. Each experiment was conducted twice and the deviation of temperature distribution maintained 10%.

As shown in **Fig. 4b**, the typical charging procedure using the back-filling process on a single charging tube OHP was employed. A vacuum pump (Leybold, D16C) was employed for filling the pipes with working fluid. The tube was charged with fluids with different filling ratios, which is defined as the ratio of working fluid volume to the total volume of the oscillating pipe. The filling ratio was controlled by the digital balance: 1) with valve 2 closed, OHP was vacuumed by the pump; 2) with valve 1 and valve 3 closed, the mass of filling into the connecting pipes was measured by the digital balance after opening valve 2; 3) with valve 3 closed, the mass of liquid filling into OHP (with filling ratio of ~100%) and the connecting pipes was measured after opening valve 1, and the mass of liquid filling into OHP with filling ratio of 100% was obtained after this three procedures; 4) with knowing the total liquid mass inside the OHP, different filling ratios were achieved by controlling valve 1 according to the measurement of mass from the digital balance.
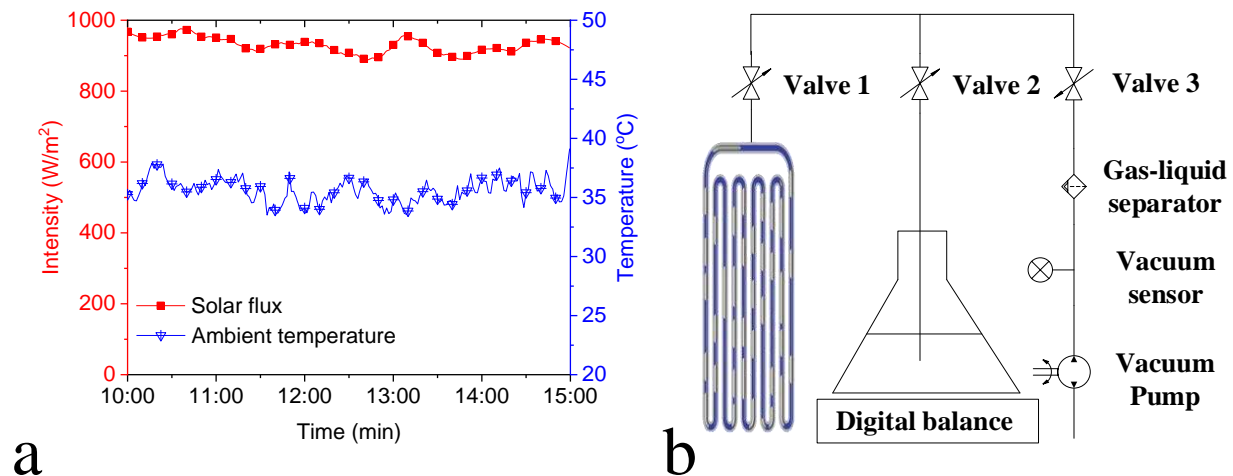
Fig. 4 (**a**) Solar intensity and ambient temperature during experiment period; (**b**) Charging system for OHP

3. Results and Discussion

3.1 Startup process

The initial pressure inside the pipe after filling the nanofluid was ~3 kPa, corresponding to a saturation temperature ~20 ℃, which was the ambient temperature (i.e., 20~25 ℃). The two-phase (liquid-vapor) exists for all OHPs in this work, which is normal for typical heat pipes due to vacuumed process. The concentration of gold nanofluid in this work is relatively low, i.e., maximum 12.5 ppm. The nanoparticles barely affect the saturated pressure. As measured by the pressure sensor, the pressure is almost the same when OHPs are filled with DI water and gold nanofluid with different concentrations. **Fig. 5** shows a typical example of the starting up process with and without nanoparticles for a liquid filling ratio of 67%. Due to the cooling water circulation, the temperature of the condenser maintained about 15 ℃. For pipes filled with DI water (**Fig. 5a**), no liquid flow was observed for the first 2 minutes after applying the concentrated sunlight. The temperature of the evaporator kept increasing and the center of the evaporator went over 100 ℃ in two minutes. There was significant temperature non-uniformity in the evaporator section, and over 70 ℃ was observed between the center and the edge of the evaporator at 120 s. A sudden temperature drop happened at ~120s, when the bubbles near the center of the heat pipe started forming and rapidly driving water flow, which indicated the startup of the bubble oscillation. However, the frequency of such bubble oscillation was low. The temperature and temperature difference among different parts of the evaporation section continued increasing until the next pulsating flow. The startup process showed intermittent appearance of liquid and bubbles, similar to a typical oscillating heat pipe at low heat flux.

For pipes filled with 5 ppm gold nanoparticles (AuNPs) (**Fig. 5b**), however, it was observed that the liquid started to flow almost instantaneously driven by randomly growing bubbles when the concentrated sunlight was applied. This resulted in a slow increase of the wall temperature at the evaporation section. The wall temperature kept increasing until the formation of large accelerating

bubbles at ~1 minute, leading to a sharp temperature decrease. Contrasting to the large temperature variation as in the DI water case, the temperature of the evaporation section was highly uniform, with a maximum 5 ℃ difference. Smooth startup and active response to concentrated sunlight were observed during the whole experiment period. It was noted that there was distinct temperature difference between adjacent pipes in the adiabatic section of the solar collector (i.e. between the evaporator and the condenser), as shown in **Fig. 5b** inside infrared images. This is resulted from the circular movement of the liquid slugs, i.e., the generation of upward bubbles was associated with downflow of liquid slugs in adjacent pipes.
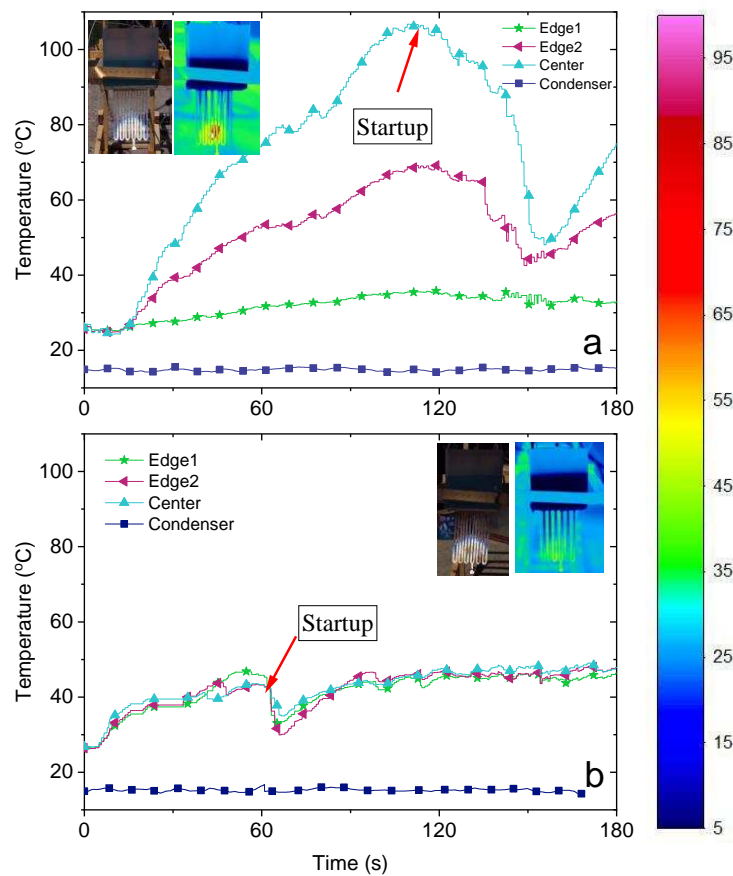
Fig. 5 Temperature variation of the evaporator and condenser section: (**a**) and (**b**) filling with of DI water and gold nanofluid with concentartion of 5 ppm, respectively. The filling ratio is 67%.

The inset shows the photos and infrared images taken at 60 s after applying concentrated solar radiation. **Edge1** represents the average temperature of the evaporator section of pipe 1, 2, 11, 12; **Edge2** represents the average temperature of pipe 3, 4, 9, 10; **Center** represents the average temperature of pipe 5, 6, 7, 8; **Condenser** reperesents the average temeprature of the two thermocouples attached to the condenser inside the cooling water.

The reason for such big difference is associated with increased solar energy absorption by nanoparticles and subsequent generation of bubbles. Many studies have shown that the addition of small concentrations of nanoparticles could increase solar energy absorption significantly [36], especially for gold nanoparticles. Due to the effect of the Beer's law [37], the absorbed solar energy is concentrated at the surface area, leading to local high temperature that allows strong bubble generation in the evaporation section, which initiates fluid circulation, achieving much higher heat transfer performance. There have been many discussions on the mechanism of heat transfer improvement by nanoparticles. Clearly for this work, the improvement of heat transfer is not due to the effect of slightly increased thermal conductivity, nor purely the nanoparticles effect associated with conventional OHPs (i.e., heating to metallic evaporation section). The harvested solar energy by nanoparticles that leads to stable generation of bubbles at the evaporation session is the main reason.

It was noted that for 5 ppm AuNPs fluid oscillation with intermittent circulation and flow reversals, indicated by 'flow direction switch' [24,38], was observed. The bubbles motion was close to a quasi-steady state, without large bubble accelerations. We classified this motion as the first mode in this work, i.e., random generation of bubbles under low heat fluxes with small accelerations, accompanied by occasional flow reversals. As shown in **Supplementary Video** (First mode), with the bubbles growing, some liquid slugs could possibly run into the condensation

section. However, due to the slow generation of small bubbles and the frequent switch of flow direction, the newly generated bubbles were difficult to reach the condensation section, which could limit the heat transfer efficiency of the OHPs. It has been shown that fluid running in one-way direction is the most efficient heat transfer model, as investigated below.

3.2 Effect of nanoparticle concentration

Controlled experiments were carried out for different concentrations of nanofluid, as shown in **Fig. 6**. The performance of 7.5 ppm, as shown in **Fig. 6a**, was very similar to that of 5 ppm. The non-uniform distribution of solar intensity does exist, which is due to the Fresnel lens. But for each experiment, the non-uniform distribution of solar intensity is almost the same for each experimental period (i.e., 3 minutes as shown in **Fig. 6**). So, the non-uniform supply of heat is the same for the experimental period, the variation in temperature with time is not due to the non-uniform supply of heat. The more absorption of solar energy due to increased particle concentration led to a higher liquid temperature and stronger bubble motions. Fluid oscillation was induced and a quick reach to the steady state was observed with little wall temperature non-uniformity. The fluid motion can be still well described by the first mode. However, a different phenomenon was observed for the 12.5 ppm case. Large wall temperature fluctuations in the evaporation section was observed (as shown in **Fig. 6b**), indicted by the formation of one direction fluid running inside the pipes, evidenced by the formation of large bubbles with large accelerations, i.e., the second mode. For the second mode (when the concentration of nanofluid is high), the newly generated bubbles can easily go into the condensation section due to the fast generation of large bubbles and the one-way circulation of nanofluids (as shown in **Supplementary Video**), which significantly benefit the heat transfer process of the OHPs. The occurrence of the second

mode is also intermittent, e.g., around every 40 s as shown in **Fig. 6b** for the case of 12.5 ppm. The overlapping of the first and second mode produced large temperature variations. This interesting phenomenon was associated with the forming of large accelerating bubbles due to increased solar energy capture, which provided the required pumping force to drive the fluid running in one direction. During the bubble growth period, the rapid evaporation of the liquid layer (i.e., between the bubble and the wall) needed to sustain accelerating bubbles, would cause the dry out phenomenon [39], leading to a large temperature increase. The departure of the large bubble was followed by the influx of liquid slugs, which cooled down the wall subsequently, thus forming large temperature fluctuations in a quasi-sine mode. This phenomenon is very similar to those confined bubble movement observed in flow boiling in narrow channels [40].

There were speculations that nanobubbles could be formed around heated nanoparticles under focused solar light, and subsequent merger of these nanobubbles would produce large bubbles [41,42]. We have shown in our previous work that the hypothesis of nanobubbles was not valid [5]. Strong evaporation was mainly caused by localized boiling and evaporation in superheated regimes due to a highly non-uniform temperature distribution, albeit the bulk fluid was still subcooled. Such a phenomenon can be explained by the classical heat transfer theory and the hypothesized 'nanobubble', i.e., steam produced around heated particles, was unlikely to occur under normal solar concentrations. The hypothesis of the modification of interfacial tension (IFT) by nanoparticles that make the bubble generation easier [43] is also not feasible. There is still strong debate if nanoparticles alone could modify the IFT, and even so, the magnitude of IFT was not sufficient to bring such big differences. It is the formation of large accelerating bubbles, i.e. the second mode, that responsible for the one-way fluid flow.
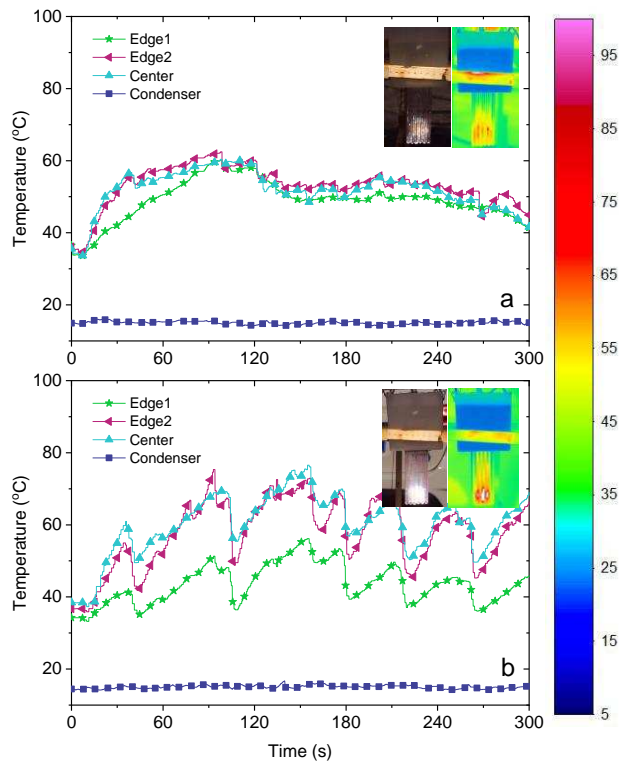
Fig. 6 Temperature variation of the evaporator section : (**a**) and (**b**) filling with of gold nanofluid with concentartion of 7.5 ppm and 12.5 ppm, respectively. The filling ratio is 67%. The inset shows the photos and infrared images taken at 60 s after applying concentrated solar radiation.

3.3 Bubble characterization and pumping force analysis

The growth and dynamic movement of bubbles were crucial to the oscillating and heat transfer performance of the OHP. A typical flow regime variation within 0.39 s for DI water and 12.5 ppm gold nanofluid were shown in **Fig. 7**. The main observation can be concluded as follow:

1) The average bubble size was small for DI water after the startup, i.e. in the range of 2 ~5 mm, except for a few growing large bubbles as shown in **Fig. 7a**. For the nanofluid, however the bubble

size was in the regime of 3 ~8 cm, and most of them had long journey movement that passing from evaporation section to the condensation section, as shown in **Fig. 7b**.

2) The movement of bubbles for DI water was slow, and difficult to circle in one direction, accompanied by occasional flow reversal. Most of the bubbles only slightly moved upward with a low velocity ~ 0.015 m/s, which was calculated through the bubble's positions captured by the camera. Some even showed no movement. The lack of fast movement of bubbles limited the heat transfer performance of OHP, which resulted in the high temperature of evaporation section as shown in **Fig. 5a**. For the nanofluid, however, the movement was more violent. The example shown in **Fig. 7b** had a bubble velocity of 0.25 m/s, leading to one direction flow (i.e., the bubbles inside every two pipes moved to the same direction, upward as marked in **Fig. 7b**). This initiated the second flow mode, consistent with the findings of 'flow direction switch' phenomenon.

3) Newly formed bubbles had large accelerations for nanofluid samples. For the example shown in red dotted line in T+0.39 s, **Fig. 7b**, newly generated bubbles pushed the previous bubbles into the condensation section, driven by other newly generated ones. A new bubble grew to as much as about 10 cm within 0.13 s, i.e. having an average bubble velocity of ~0.7 m/s. The rapid bubble generation and movement not only accelerate the heat transfer process, but also create a relative high pressure inside pipes, contributing to the latent heat release inside the condensation section.
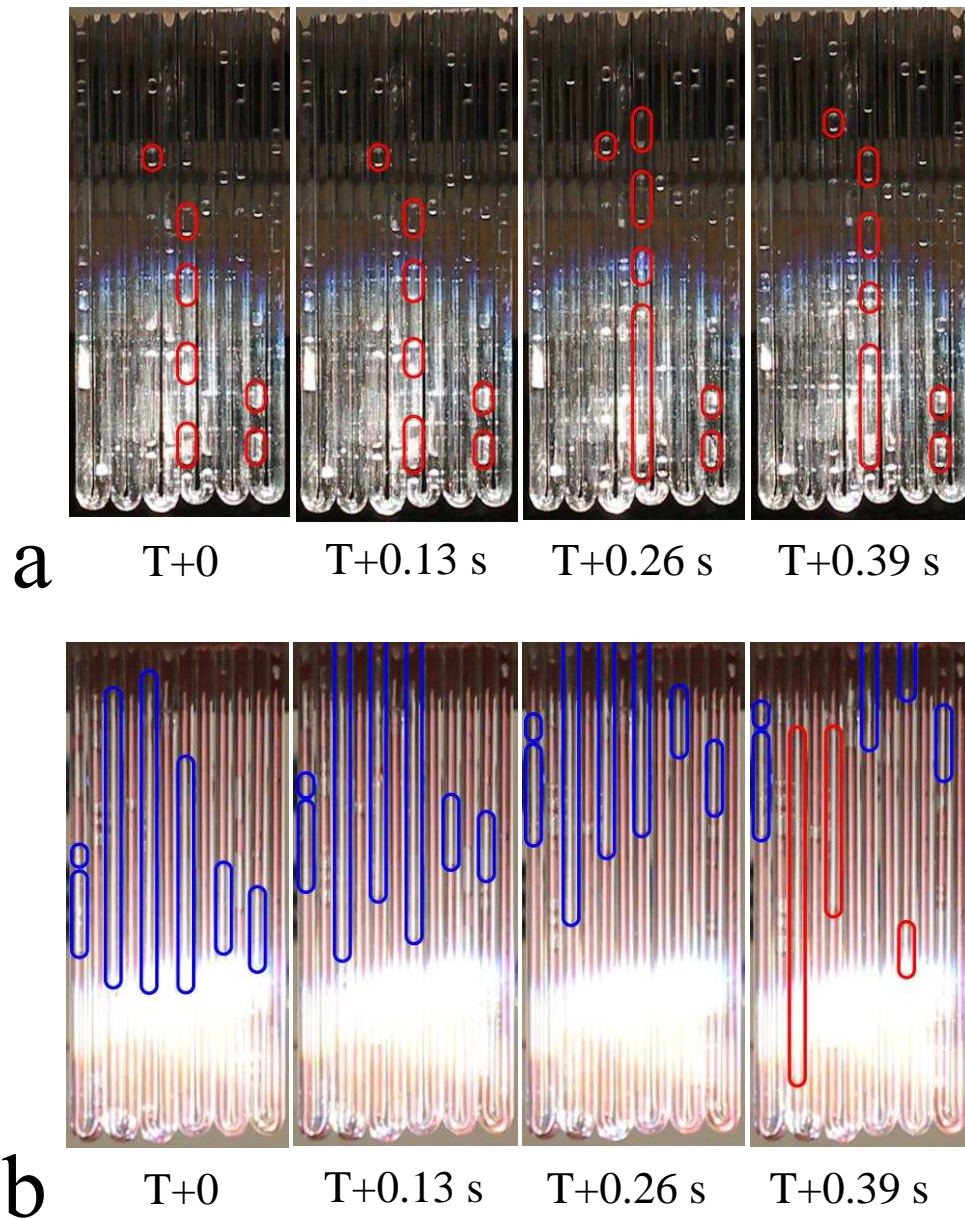
Fig. 7 Bubble growth and dynimic movement within 0.39 s of DAS-OHP filled with DI water (**a**) and gold nanofluid (**b**) with filling ratio of 67%. The bubble was marked for every other pipes.

It is believed that the unique characteristics of bubble motions were closely related to the absorbed solar energy. At a low particle concentration, the flow was in the first mode due to low solar energy absorption. The dominant flow pattern of the working fluid was the slug flow when the heat pipe was started, resulting in random oscillation of the working fluid at low velocity (**Fig.**

6a). However, at a high particle concentration (**Fig. 6b**), the flow was the overlapping of the first and second motion due to more absorbed solar energy. Vigorous bubble generation would occur at the evaporation section, where the flow pattern might change to semi-annular flow and even the annular flow [44].

To estimate the momentum motivated by oscillating bubbles, the average accelerations of oscillating bubbles were estimated from transient movement of bubbles within an oscillating period. Clearly the acceleration of the solar absorber filled with gold nanofluid was much higher. The bubble acceleration at 12.5 ppm nanofluid reached as much as 2.24 m/s^2, which was almost 18 times of that of DI water sample (0.14 m/s^2). The average pumping force from oscillating bubbles was estimated from the acceleration according to the following equation,

$$F_{pumping} = \theta m_{max} a \tag{1}$$

where a is the acceleration, θ and m_{max} were the filling ratio and the maximum filling mass of working fluid, respectively. Assuming an ideal case that no frictional force from the inner surface, the maximum pumping force for the case of 12.5 ppm nanofluid was obtained as 0.056 N, which is sufficient to transfer fluids from the evaporator to the condenser.

3.4 Energy and thermal resistance analysis

Similar to OHPs, thermal resistance was used to quantify the performance of different cases studied in this work. The photothermal conversion efficiency needs to be firstly calculated. Our previous work [5,13] showed that nanoparticles inside the fluid scatter solar light independently, and the absorption and scattering coefficients could be calculated based on the Mie theory. The absorbed solar energy by the solar collector can be calculated:

$$Q_{abs} = \eta_{fv}\eta_l I S_l \tag{2}$$

where η_l is efficiency of Fresnel lens (a typical value of 92% has been chosen), η_{f_v} is the photothermal conversion efficiency calculated from **Supplementary Note**, I is the solar intensity when experimenting (measured by solar intensity sensor, a typical value of 1000 W/m²), and S_l is the area of the Fresnel lens.

The thermal resistance of the collector can be calculated from [45]:

$$R_{OHP} = \frac{\bar{T}_e - \bar{T}_c}{Q_{abs}} \tag{3}$$

where $\bar{T}_e$ and $\bar{T}_c$ are the average temperature of evaporator and condenser.

The thermal resistances were calculated based on experimental data for different filling ratios and particle concentrations, as shown in **Fig. 8**. It showed clearly that solar collector filled with nanofluid could significantly decrease the thermal resistance, which is due to increased solar absorption and enabled bubble dynamics. Among all the fluids tested, 12.5 ppm AuNPs nanofluid had the smallest thermal resistance, i.e., ~10 times smaller than that of DI water. Clearly both experiments and predictions showed that there was a minimum resistance value for a given filling ratio (e.g., 0.38 K/W at a filling ratio of 92% for 7.5 ppm AuNPs; 0.14 K/W at a filling ratio of 83% for 12.5 ppm AuNPs). The initial distribution of liquid and vapor slugs depends on the filling ratio, which shall have significant influence on the performance of OHP. For a low filling ratio, liquid can be easily dried out at the evaporation section, resulting in poor performance, similar to conventional OHPs [23]. A very high filling ratio, however, would also deteriorate the performance of OHP due to the existence of long liquid slugs and hence low vapor acceleration. Han et.al [46] concluded from previous works [47,48] that there was an "optimal range" for filling ratio, which was in the region of 35%-65%. In this work, however, we showed that the optimum filling ratio was higher than 65%, whose value increased with the increase of nanoparticle concentration. This is due to the dependence of absorbed solar energy flux on the nanoparticle

concentration. A higher nanoparticle concentration captured more solar energy (i.e., as much as $40W/cm^2$ for gold nanofluid that is much higher than previous studies), and evaporated the liquid faster, which requires more liquid to sustain the evaporation at the optimum condition, leading to a higher optimal filling ratio. Increasing filling ratio value would lead to quasi-sine oscillations, as shown in **Fig. 6b** and **Fig. 7**. These sinusoidal oscillations were originated from regular oscillating motions and were only available at suitable power inputs and filling ratios, i.e., higher than 67% in this study.
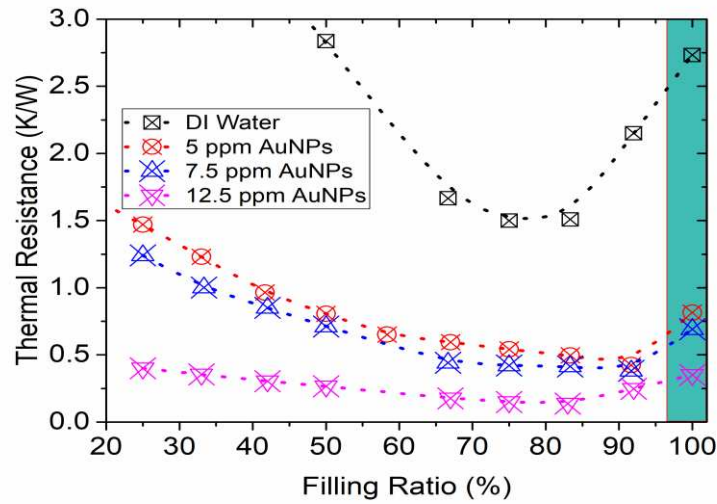
Fig. 8 Variation of thermal resistance with filling ratio for DAS-OHP filled with AuNPs nanofluid with different concentrations.

The inner diameter of the OHP must be small enough (e.g., 2 mm in this paper) so that vapor plugs and liquid slugs can be formulated due to the dominant effect of the surface tension of the working fluid, which seriously limits the absorbance of solar energy for the OHP. For instance, according to **Eq. 2**, the photo-thermal conversion efficiency (PTE) in this work is 8.57%, 19.03% and 29.83% for the OHP filled with DI water, 5 ppm and 12.5 ppm gold nanofluids with the filling ratio of 100%, respectively, which means that most of the solar energy will penetrate the OHP due

to thin optical depth. According to our previous study [13], PTE is very sensitive when the optical depth is below 20 mm, where PTE increases quickly with increasing optical depth. For an optical depth of 2 mm (i.e., the diameter of the tube), the PTE for a pure fluid is in a very small range (< 10%), which significantly limits the performance of the OHP. However, the PTE of the OHP can reach very high when the tubes are filled with multi-wall carbon nanotube (MWCNT) nanofluid with high concentration of 3.0 wt% (from **Supplementary Note**). The maximum efficiency of OHP filled with MWCNTs nanofluid is around 92%, which is much higher than those reported the maximum solar thermal efficiency of a plate solar collector with glazed copper OHP. Two independent work showed that the maximum efficiency were 62% [49] and 53.79% [29] respectively. This high efficiency is due to a few reasons, including 1) high heat transfer process under concentrated solar intensity, where the OHP progresses intensively and achieves an effective thermal conductivity of 6000 W/(m · K); 2) low level of heat leak due to the volumetric absorption of nanofluid inside the OHP by the 'thermal trapping' effect [5,13], i.e., the highest temperature exists inside the nanofluid instead of on the surface for plate solar collectors; and 3) the compact arrangement of transparent OHP tubes that absorb most of the solar energy, more efficient than most of vacuum-tube solar collector (i.e., there is typically large gap between adjacent vacuum-tubes due to the nature of the install panel, which wastes nearly 30% of the irradiated area). The maximum efficiency for evacuated head pipes is typically less than 70% if the gap area is considered. Not only the efficiency, the proposed system has many other advantages such as low cost and easy manufacturing.

4. Conclusions

This work validated experimentally the innovative idea of a pump-free solar collector concept by using direct absorption nanoparticles for efficient solar energy harvesting. The results show that

by using direct absorption gold nanoparticles, much higher amount of solar energy can be captured that allows a vigorous generation of bubbles, which enables the circulation of fluids between the evaporator and the condenser, and efficient transport of energy without using extra pumping power. The performance is however related to particle concentration and filling ratio. Different flow modes can be formed at different nanoparticle concentrations, and there is an optimum filling ratio to reach the minimum thermal resistance. Further optimization of the system is recommended on proper selection of nanoparticle type and nanoparticle concentration.

Author contributions

D. W. originated the idea and supervised the work. The manuscript was written through contributions of all authors. H. J. and Y. G. performed experiments and simulation under instructions, G. L. provided supervision for the work in Beihang University, D. W. revealed bubble generation mechanisms and provided overall quality control. All authors have given approval to the final version of the manuscript.

Competing interests

The authors declare no competing financial interests.

Supplementary information

     I.   **Video showing bubble generation and increase of first mode**

    II.   **Video showing bubble generation and increase of second mode.**

   III.   **Supplementary figure and note**

Reference

[1]   S. Chu, A. Majumdar, Opportunities and challenges for a sustainable energy future, Nature. 488 (2012) 294–303. doi:10.1038/nature11475.

[2]   N.S. Lewis, Research opportunities to advance solar energy utilization, Science (80-.). 351 (2016) aad1920-aad1920. doi:10.1126/science.aad1920.

[3]   R. Service, Microbe-linked solar panels are better than plants at converting sunlight to energy, Science (80-.). (2016). doi:10.1126/science.aag0586.

[4]   A. Lenert, E.N. Wang, Optimization of nanofluid volumetric receivers for solar thermal energy conversion, Sol. Energy. 86 (2012) 253–265. doi:10.1016/j.solener.2011.09.029.

[5]   H. Jin, G. Lin, L. Bai, A. Zeiny, D. Wen, Steam generation in a nanoparticle-based solar receiver, Nano Energy. 28 (2016) 397–406. doi:10.1016/j.nanoen.2016.08.011.

[6]   K. Khanafer, K. Vafai, A review on the applications of nanofluids in solar energy field, Renew. Energy. 123 (2018) 398–406. doi:10.1016/j.renene.2018.01.097.

[7]   A. Gimeno-Furio, L. Hernandez, N. Navarrete, R. Mondragon, Characterisation study of a thermal oil-based carbon black solar nanofluid, Renew. Energy. 140 (2019) 493–500. doi:10.1016/j.renene.2019.03.080.

[8]   X. Jin, G. Lin, A. Zeiny, H. Jin, L. Bai, D. Wen, Solar photothermal conversion characteristics of hybrid nanofluids: An experimental and numerical study, Renew. Energy. 141 (2019) 937–949. doi:10.1016/j.renene.2019.04.016.

[9]   R. Loni, E.A. Asli-Ardeh, B. Ghobadian, A.B. Kasaeian, S. Gorjian, G. Najafi, E. Bellos, Research and review study of solar dish concentrators with different nanofluids and different shapes of cavity receiver: Experimental tests, Renew. Energy. (2019). doi:10.1016/j.renene.2019.06.056.

[10]   B. V. Balakin, O. V. Zhdaneev, A. Kosinska, K. V. Kutsenko, Direct absorption solar collector with magnetic nanofluid: CFD model and parametric analysis, Renew. Energy. 136 (2019) 23–32. doi:10.1016/j.renene.2018.12.095.

[11]   M.A. Sharafeldin, G. Gróf, Efficiency of evacuated tube solar collector using WO3/Water nanofluid, Renew. Energy. 134 (2019) 453–460. doi:10.1016/j.renene.2018.11.010.

[12]   V. Khullar, H. Tyagi, N. Hordy, T.P. Otanicar, Y. Hewakuruppu, P. Modi, R.A. Taylor, Harvesting solar thermal energy through nanofluid-based volumetric absorption systems, Int. J. Heat Mass Transf. 77 (2014) 377–384. doi:10.1016/j.ijheatmasstransfer.2014.05.023.

[13] H. Jin, G. Lin, L. Bai, M. Amjad, E.P. Bandarra Filho, D. Wen, Photothermal conversion efficiency of nanofluids: An experimental and numerical study, Sol. Energy. 139 (2016) 278–289. doi:10.1016/j.solener.2016.09.021.

[14] H. Jin, G. Lin, A. Zeiny, L. Bai, D. Wen, Nanoparticle-based solar vapor generation: An experimental and numerical study, Energy. 178 (2019) 447–459. doi:10.1016/j.energy.2019.04.085.

[15] H.K. Gupta, G. Das Agrawal, J. Mathur, An experimental investigation of a low temperature Al2O3-H2O nanofluid based direct absorption solar collector, Sol. Energy. 118 (2015) 390–396. doi:10.1016/j.solener.2015.04.041.

[16] J. Pérez-Juste, I. Pastoriza-Santos, L.M. Liz-Marzán, P. Mulvaney, Gold nanorods: Synthesis, characterization and applications, Coord. Chem. Rev. 249 (2005) 1870–1901. doi:10.1016/j.ccr.2005.01.030.

[17] S. Eustis, M.A. El-Sayed, Why gold nanoparticles are more precious than pretty gold: Noble metal surface plasmon resonance and its enhancement of the radiative and nonradiative properties of nanocrystals of different shapes, Chem. Soc. Rev. 35 (2006) 209–217. doi:10.1039/B514191E.

[18] H. Ghasemi, G. Ni, A.M. Marconnet, J. Loomis, S. Yerci, N. Miljkovic, G. Chen, Solar steam generation by heat localization, Nat. Commun. 5 (2014) 4449. doi:10.1038/ncomms5449.

[19]   S. Yu, Y. Zhang, H. Duan, Y. Liu, X. Quan, P. Tao, W. Shang, J. Wu, C. Song, T. Deng,

         The impact of surface chemistry on the performance of localized solar-driven evaporation

         system, Sci. Rep. 5 (2015) 13600. doi:10.1038/srep13600.

[20]   O. Mahian, L. Kolsi, M. Amani, P. Estellé, G. Ahmadi, C. Kleinstreuer, J.S. Marshall,

         R.A. Taylor, E. Abu-Nada, S. Rashidi, H. Niazmand, S. Wongwises, T. Hayat, A.

         Kasaeian, I. Pop, Recent advances in modeling and simulation of nanofluid flows—Part

         II: Applications, Phys. Rep. 791 (2019) 1–59. doi:10.1016/J.PHYSREP.2018.11.003.

[21]   O. Mahian, L. Kolsi, M. Amani, P. Estellé, G. Ahmadi, C. Kleinstreuer, J.S. Marshall, M.

         Siavashi, R.A. Taylor, H. Niazmand, S. Wongwises, T. Hayat, A. Kolanjiyil, A. Kasaeian,

         I. Pop, Recent advances in modeling and simulation of nanofluid flows-Part I:

         Fundamentals and theory, Phys. Rep. 790 (2019) 1–48.

         doi:10.1016/J.PHYSREP.2018.11.004.

[22]   H. Akachi, United States Patent: 4921041-Structure of a heat pipe, 1990.

[23]   J. Qu, X. Li, Y. Cui, Q. Wang, Design and experimental study on a hybrid flexible

         oscillating heat pipe, Int. J. Heat Mass Transf. 107 (2017) 640–645.

         doi:10.1016/j.ijheatmasstransfer.2016.11.076.

[24]   Q. Sun, J. Qu, X. Li, J. Yuan, Experimental investigation of thermo-hydrodynamic

         behavior in a closed loop oscillating heat pipe, Exp. Therm. Fluid Sci. 82 (2017) 450–458.

         doi:10.1016/j.expthermflusci.2016.11.040.

[25]   A.A. Hathaway, C.A. Wilson, H.B. Ma, Experimental Investigation of Uneven-Turn
        Water and Acetone Oscillating Heat Pipes, J. Thermophys. Heat Transf. 26 (2012) 115–
        122. doi:10.2514/1.T3734.

[26]   C.Y. Tseng, K.S. Yang, K.H. Chien, M.S. Jeng, C.C. Wang, Investigation of the
        performance of pulsating heat pipe subject to uniform/alternating tube diameters, Exp.
        Therm. Fluid Sci. 54 (2014) 85–92. doi:10.1016/j.expthermflusci.2014.01.019.

[27]   H. Xian, W. Xu, Y. Zhang, X. Du, Y. Yang, Experimental investigations of dynamic fluid
        flow in oscillating heat pipe under pulse heating, Appl. Therm. Eng. 88 (2015) 376–383.
        doi:10.1016/j.applthermaleng.2014.12.019.

[28]   S.H. Kargar, M. Ghiasei, M. Mirzaei, R.S. Nejad, Experimental Investigation of the Effect
        of Using Pulsating Heat Pipes on the Performance of a Solar Air Heater, Int. Conf. Mech.
        Electr. Technol. 3rd, (ICMET-London 2011), Vol. 1–3. 75 (2011) 501–507.
        doi:10.1115/1.859810.paper377.

[29]   M. Arab, M. Soltanieh, M.B. Shafii, Experimental investigation of extra-long pulsating
        heat pipe application in solar water heaters, Exp. Therm. Fluid Sci. 42 (2012) 6–15.
        doi:10.1016/j.expthermflusci.2012.03.006.

[30]   H. Kargarsharifabad, S.J. Mamouri, M.B. Shafii, M.T. Rahni, Experimental investigation
        of the effect of using closed-loop pulsating heat pipe on the performance of a flat plate
        solar collector, J. Renew. Sustain. Energy. 5 (2013). doi:10.1063/1.4780996.

[31]   R.J. Xu, X.H. Zhang, R.X. Wang, S.H. Xu, H.S. Wang, Experimental investigation of a
        solar collector integrated with a pulsating heat pipe and a compound parabolic

concentrator, Energy Convers. Manag. 148 (2017) 68–77.

doi:10.1016/j.enconman.2017.04.045.

[32]   Z.-H. Liu, Y.-Y. Li, R. Bao, Compositive effect of nanoparticle parameter on thermal

performance of cylindrical micro-grooved heat pipe using nanofluids, Int. J. Therm. Sci.

50 (2011) 558–568. doi:10.1016/j.ijthermalsci.2010.11.013.

[33]   S. Rittidech, A. Donmaung, K. Kumsombut, Experimental study of the performance of a

circular tube solar collector with closed-loop oscillating heat-pipe with check valve

(CLOHP/CV), Renew. Energy. 34 (2009) 2234–2238. doi:10.1016/j.renene.2009.03.021.

[34]   H. Chen, D. Wen, Ultrasonic-aided fabrication of gold nanofluids, Nanoscale Res. Lett. 6

(2011) 198. doi:10.1186/1556-276X-6-198.

[35]   H. Zheng, S. Chang, Y. Zhao, Anti- Icing ＆ Icephobic Mechanism and Applications of

Superhydrophobic / Ultra Slippery Surface ＊ ＊, (2017). doi:10.7536/PC161015.

[36]   K. Bae, G. Kang, S.K. Cho, W. Park, K. Kim, W.J. Padilla, Flexible thin-film black gold

membranes with ultrabroadband plasmonic nanofocusing for efficient solar vapour

generation, Nat. Commun. 6 (2015) 10103. doi:10.1038/ncomms10103.

[37]   M.F. Modest, Radiative Heat Transfer, Academic Press, 2003.

doi:http://dx.doi.org/10.1016/B978-012503163-9/50021-7.

[38]   J.L. Xu, Y.X. Li, T.N. Wong, High speed flow visualization of a closed loop pulsating

heat pipe, Int. J. Heat Mass Transf. 48 (2005) 3338–3351.

doi:10.1016/j.ijheatmasstransfer.2005.02.034.

[39]   J.R. Thome, V. Dupont, A.M. Jacobi, Heat transfer model for evaporation in microchannels. Part I: Presentation of the model, Int. J. Heat Mass Transf. 47 (2004) 3375–3385. doi:10.1016/j.ijheatmasstransfer.2004.01.006.

[40]   D. Wen, Flow boiling heat transfer in microgeometries, Doctoral dissertation, University of Oxford, 2004. http://ethos.bl.uk/OrderDetails.do?uin=uk.bl.ethos.414305 (accessed March 20, 2018).

[41]   O. Neumann, A.S. Urban, J. Day, S. Lal, P. Nordlander, N.J. Halas, Solar vapor generation enabled by nanoparticles, ACS Nano. 7 (2013) 42–49. doi:10.1021/nn304948h.

[42]   O. Neumann, C. Feronti, A.D. Neumann, A. Dong, K. Schell, B. Lu, E. Kim, M. Quinn, S. Thompson, N. Grady, P. Nordlander, M. Oden, N.J. Halas, Compact solar autoclave based on steam generation using broadband light-harvesting nanoparticles, Proc. Natl. Acad. Sci. 110 (2013) 11677–11681. doi:10.1073/pnas.1310131110.

[43]   S.J. Kim, I.C. Bang, J. Buongiorno, L.W. Hu, Surface wettability change during pool boiling of nanofluids and its effect on critical heat flux, Int. J. Heat Mass Transf. 50 (2007) 4105–4116. doi:10.1016/j.ijheatmasstransfer.2007.02.002.

[44]   L. Jia, Y. Li, Experimental Research on Heat Transfer Characteristics of Pulsating Heat Pipe, Heat Transf. Vol. 2. (2008) 375–379. doi:10.1115/HT2008-56203.

[45]   T. Hari Prasad, P.R. Kukutla, P. Mallikarjuna Rao, R.M. Reddy, Experimental Investigation on Performance of Pulsating Heat Pipe, ASME 2015 Gas Turbine India Conf. 45 (2015) V001T04A005. doi:10.1115/GTINDIA2015-1362.

[46]   X. Han, X. Wang, H. Zheng, X. Xu, G. Chen, Review of the development of pulsating heat pipe for heat dissipation, Renew. Sustain. Energy Rev. 59 (2016) 692–709. doi:10.1016/j.rser.2015.12.350.

[47]   H.-S. Jeong, J.-H. Kim, J.-W. Kim, J.-S. Kim, The Study on Pressure Oscillation and Heat Transfer Characteristics of Oscillating Capillary Tube Heat Pipe Using Mixed Working Fluid, Trans. Korean Soc. Mech. Eng. B. 26 (2002) 318–327. doi:10.3795/KSME-B.2002.26.2.318.

[48]   M. Vassilev, Y. Avenas, C. Schaeffer, J.L. Schanen, J. Schulz-Harder, Experimental study of a pulsating heat pipe with combined circular and square section channels, Conf. Rec. - IAS Annu. Meet. (IEEE Ind. Appl. Soc. (2007) 1419–1425. doi:10.1109/IAS.2007.219.

[49]   K.B. Nguyen, S.H. Yoon, J.H. Choi, Effect of working-fluid filling ratio and cooling-water flow rate on the performance of solar collector with closed-loop oscillating heat pipe, J. Mech. Sci. Technol. 26 (2012) 251–258. doi:10.1007/s12206-011-1005-8.